Influence of an active T-foil on motions and passenger comfort of a wave-piercing catamaran based on sea trials in oblique seas

C. Y. Lau,[1] J. Ali-Lavroff, [1] D. S. Holloway, [1] J. A. Mehr, [1] G. Thomas[2]
([1]University of Tasmania, [2]University College London)

Abstract

In this paper the influence of a Ride-Control System (RCS) on the Response Amplitude Operator (RAO) of a full-scale high-speed catamaran was investigated using sea trials data. A T-foil and stern tabs were installed on a Wave-Piercing Catamaran (Incat Tasmania Hull 061) to improve ship motions and passenger comfort. More than 40 total effective hours of sea trials were conducted by the US Navy in 2004, encountering sea states 4 to 5 in the Atlantic Ocean near the United Kingdom.

The reduction in Motion Sickness Incidence (MSI) was estimated in order to examine the effectiveness of the RCS in improving passenger comfort. By comparing the case of active RCS (T-foil plus stern tabs) with the case of active stern tabs only, it was found that the T-foil plays a vital role in the passenger comfort enhancement. Based on ISO recommended MSI calculation of a 2-hour seaway, the percentage reduction in MSI was estimated, and hence the effectiveness of the T-foil deployment, along with the influence of speeds, headings, location on board and encountered wave height were analysed.

A notable improvement in passenger comfort was observed in the real world bow quartering sea by deploying the RCS. An MSI reduction of 21% in high speeds (30-35 knots, Fr≈0.6) was observed, which was almost twice the MSI reduction (11%) in low speeds (15-20 knots, Fr ≈ 0.3). However, in terms of MSI percentage reduction, the ability of T-foil in vessel motion control in oblique seas was found to be limited compared to the results in head seas.

1 Introduction

1.1 Background

The increasing demand for high-speed marine transportation has pushed the development of Roll-on-Roll-off (Ro-Ro) vessels towards faster and larger capacity. In high-speed vessels, the catamaran is often a popular option, owing to its large deck area, low wave-making resistance and high transverse stability [1-3].

To determine the operability or seaworthiness of a vessel, it is important to understand its motion while encountering waves. The most common indicator of the vessel motion is the Response Amplitude Operator (RAO), which can represent the motion response under various wave frequencies [4-12], though the response is somewhat non-linear to the encountered waves [13-16]. Moreover, to compare the vessel motion response and further quantify passenger comfort, Motion Sickness Incidence (MSI) is analysed.

Figure 1: 98 m Incat Tasmania Hull 061 WPC HSV-2 Swift [17]

The study of MSI was first carried out by O'Hanlon and McCauley [18], exposing humans to vertical accelerations. In their follow up research in 1976, M. E. McCauley et al. suggested that MSI is a function of frequency and amplitude of vertical periodical motion [19]. They found that unacclimatised humans are particularly susceptible to motion sickness (i.e., vomiting), while exposed to the vibration frequency of about 0.2 Hz. Many studies have also applied MSI as the assessment method of passenger comfort on monohulls [10, 20-23], in addition to catamarans [5, 15, 24].

Among the large number of studies focused on vessel motion response, much research was based on numerical analysis, e.g., Davis [5] analysed RAO and MSI based on the two-dimensional green function time-domain strip theory (BEAMSEA) code; and He, Castiglione [25] predicted RAO of a high-speed Delft catamaran by using the computational simulator CFDShip-Iowa. Besides theoretical approaches, experimental model tests are another common method to examine the vessel motion response, for instance,

AlaviMehr, Lavroff [26] assessed the RAO of a 2.5 m model of WPC in regular head waves.

Although there has been some research based on full-scale sea trials, none focused on passenger comfort by analysing the vessel motion response to the encountered waves. For example, Gahlinger [27] determined a motion sickness score based on the questionnaires collected from 260 cruises passengers. Almallah, Lavroff [28] studied wave response in the sea trial of the vessel HSV-2 Swift (Figure 1), but only to determine the motions and structural loads. In contrast, the present study aims to improve the understanding of vessel motion in random seas and their impact on motion sickness incidence (MSI), based on sea trials data. This may assist future design for these types of vessels.

1.2 Wave-Piercing Catamarans (WPCs)

To enhance the maximum speed and operability in rough weather, Wave-Piercing Catamaran's (WPC) were developed by Incat Tasmania. This type of vessel provides a fast, efficient, and economical marine transportation solution for both commercial and military use [3, 11, 29]. On top of the conventional catamaran hull, piercing bow edges on the demi-hulls were added to reduce wave response [30], as well as a centre bow to provide reserve buoyancy and minimise deck diving [31-34]. The piercing edges and centre bow of the WPC 'HSV-2 Swift', being central to the present study, are shown in Figure 1.

According to Fang and Chan [15], compared to conventional catamarans, WPCs show excellent seakeeping performance in oblique seas, and avoid the tendencies of bow diving in following waves reported on conventional catamarans, based on their model test and numerical results of a 41 m WPC at 20 knots. Incat Tasmania, the leading designer and manufacturer of aluminium WPCs, aims to develop a further understanding to develop and improve the systems that can improve passenger comfort and operability, such as Ride-Control Systems (RCS) and the use of the centre bow [5, 26, 32-39].

The RCS fitted on the vessels of Incat Tasmania often consists of a single retractable T-foil at the aft end of the centre bow, and two stern mounted trim tabs, as shown in Figure 2. When encountering rough seas, the RCS generates counter control forces to mitigate the vessel motions, particularly heave, pitch, and roll. In contrast, the T-foil can be retracted above the water surface to minimise drag and improve fuel efficiency when travelling in calm water.

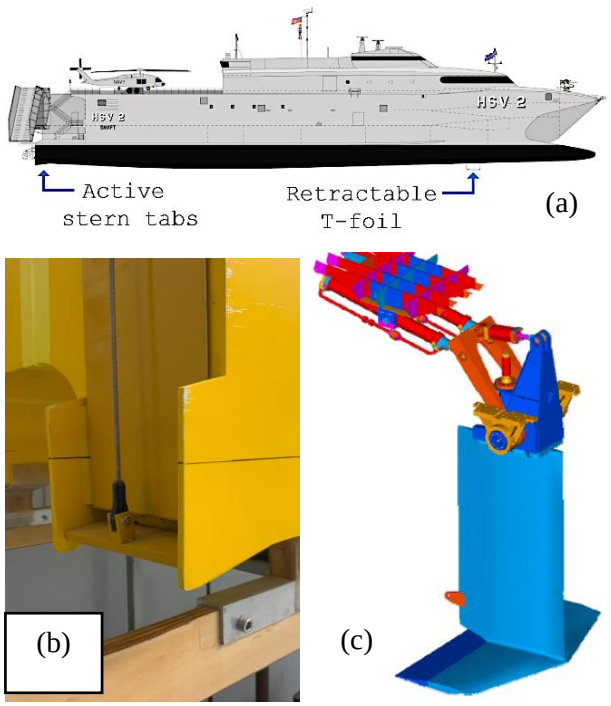

Figure 2: Incat Hull 061 - HSV-2 Swift ride-control surface (a) locations [40]; (b) example of an active stern tab on an equivalent 2.5 m Incat catamaran model [41]; (c) schematic representation of a retractable T-foil [42]

There were two adjustable angles on the T-foil of HSV-2 Swift, i.e., strut angle and flap angle. According to Smith [43], the control algorithm applied to the T-foil strut angle was proportional to pitch rate (pitch damping), while the stern tabs were controlled by 60% pitch rate and 40% of roll rate (roll damping). On the other hand, Smith reported that the control method of flap angle cannot be clearly defined from the records.

Since the T-foil was fitted at a fore location (~80% of water-line length from stern), with the assistance of stern tabs, the pitch and roll controlled actuators could limit the heave motion of the vessel [5, 26].

1.3 Motion sickness incidence of WPC fitted with RCS

As discussed in previous sections, MSI is a common indicator to assess the passenger comfort of a vessel. Therefore, to examine the effectiveness of the RCS fitted on WPCs, there have been many studies that use MSI estimation. Davis [5] predicted the MSIs during a 90-minute voyage on WPCs at the speed of 40 knots in head seas. By applying BEAMSEA code, which was developed by Davis and Holloway [44], the scenario of no RCS, tabs only, tabs and T-foil was analysed. Different control algorithms and limited slew rates were assessed. They reported a 20% reduction of MSI in 3 m waves at the fore location of the vessel using a linear control

RCS with medium slew rate, compared with the no RCS case [5]. Similarly, Zhang, Li [45] built a mathematical model of a 90 m WPC travelling at 40 knots based on strip theory, and estimated the reduction of MSI by comparing the WPC fitted with active T-foil and tabs, and without RCS. It is worth mentioning that though the predicted MSI on the centreline reduced from 19% to 5%, the estimation method of MSI they used was different from the method included in the ISO standard 2631-1 [46].

To further investigate the influence of RCS activation on passenger comfort on a WPC, this paper will present MSIs for two cases on a full-scale WPC, HSV-2 Swift, based on sea trial records. The first case is with active stern tabs only, while the second case has an active T-foil and tabs. The effect of vessel headings and speeds on MSI will first be investigated, and then the influence of wave height and encountered peak wave frequency will be studied under two different speed categories, namely low speed (15-20 knots) and high speed (30-35 knots), by fitting two regression models. Finally, the MSI in the HSV-2 Swift passenger cabin will also be predicted and plotted in a 3-D surface, along with the reduction due to T-foil deployment, to demonstrate the change of longitudinal and transverse positions on the passenger comfort in bow quartering seas.

2 HSV-2 Swift Sea trials and data collection

2.1 HSV-2 Swift

The vessel of the present study, High-Speed Vessel 2 Swift (HSV-2 Swift) is a 98 m Wave-Piercing Catamaran (WPC) designed by Revolution Design and built by Incat Tasmania (main particulars shown in Table **1**). This is the third catamaran developed for the United States Navy by Incat Tasmania.

This large aluminium vessel has a vehicle deck with total area of 2114 m^2 (22760 ft^2), with the addition of a helicopter deck to enable aircraft recovery [40]. With a cruising speed of 38 knots, and a maximum speed of 42 knots, the vessel delivered a large number of humanitarian assistance, search and rescue, and disaster relief services in a timely manner [47]. This includes support for the Tsunami that struck Southeast Asia in 2005, and the delivery of humanitarian assistance materials from Cyprus to Beirut in the Israel-Lebanon conflict during 2006.

Table 1: HSV-2 Swift main particulars [40, 48]

Length Over-All (L_{OA})	97.22 m
Length Water Line (L_{WL})	92.00 m
Draft	3.43 m
Beam	26.60 m
Demihull beam	4.50 m
Deadweight	670 tonnes
Maximum Speed	42 knots

2.2 Sea trials and data acquisition

The sea trials were conducted near the coasts of Norway and the United Kingdom, in the summer of 2004 [48]. To examine the seaworthiness and structural response of the vessel HSV-2 Swift, the trials were performed in moderate to rough seas, not commonly found in typical routes of commercial Ro-Ro ferries in service. In particular, the highest encountered significant wave height (*Hs*) was 3.7 m (Douglas Sea State 5) and the average encountered *Hs* was around 2.2 m (Douglas Sea State 4).

To record the motion and structural loads during the sea trials, instrumentation including accelerometers, a wave height radar, and other sensors, were installed on the vessel. Four three-axis accelerometers were located on the centreline at the bow, bridge, Longitudinal Centre of Gravity (LCG) and flight deck. All the accelerometers operated with a sampling frequency of 100 Hz, which was appropriate since the frequencies of interest for motion and excitation were below 1 Hz. The heave motion discussed in the present study was calculated based on the vertical acceleration measured. Inclinometers were also fitted to monitor pitch and roll of the vessel at the LCG [48, 49].

The wave height was required to enable comparison of records in similar sea states. The encountered wave was monitored by the wave height meter WM-2, designed by the Tsurumi Seiki Co., Ltd. (TSK). It was installed at the bow to sample the wave profile before interacting with the hull. This microwave doppler radar was engineered to measure the wave height from an unstable platform, such as a moving ship, with relative displacement compensation [50].

The trials comprised of runs in 21 ‘half’ octagons, each encountering a various combination of wave height, spectrum, advancing speed, and state of T-foil deployment. In general, every ‘half’ octagon included five legs, which comprised the five headings of head seas, bow-quartering seas, beam seas, stern-quarterings seas, and following seas, as shown in **Figure 3**. About half of the trials were completed by manoeuvring to port side by 45°, while the rest were accomplished by turning to starboard.

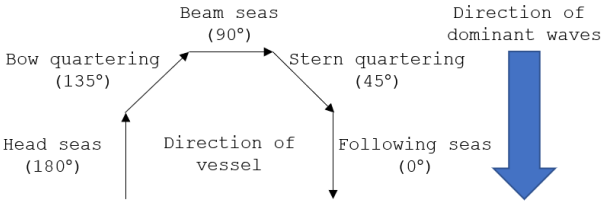

Figure 3: Typical sea trial manoeuvre pattern.

The typical procedure of the trials starts with the visual observation of the wave direction. The dominant wave direction was recorded, as well as secondary wave and swell if they existed. Then HSV-2 Swift was turned to head seas and maintained velocity until steady, after that all the instruments on board started recording. In general, the speed and course were maintained for 20 minutes in head seas, 30 minutes in beam seas, and 40 minutes in following sea, to encounter sufficient waves for maintaining statistical accuracy. After all of the legs of the trial were completed, the data collection under this particular wave height, speed and RCS status, i.e. T-foil with tabs or stern tabs only, was considered to be complete [48]. In total, more than 40 effective hours of data were recorded throughout the sea trials undertaken specifically by the Naval Surface Warfare Centre Carderock Division (NSWCCD).

2.3 Method of data analysis

To understand the hull motions and its effect on passenger comfort when encountering waves, and hence to identify the influences of factors, such as headings, RCS, speed, and waves, the present study focused on heave motions (based on measured vertical acceleration) along with pitch and roll motions at the LCG. This study starts with analysing the effect of T-foil deployment on heave, pitch and roll RAOs, at high speed (30-35 knots) and low speed (15-20 knots). The next step was to investigate the influence of headings (head seas and oblique seas) and speeds on the estimated MSI, which are presented in polar plots. Then the impact of wave excitation (significant wave height and encountered peak wave frequency) on MSI is modelled by regression. Lastly the MSI across the passenger cabin at the speed of 35 knots, is presented along with the reduction due to the T-foil operation.

The significant wave height (*Hs*) is defined as equation (1), to determine the sea state of each record.

$$Hs = 4\sqrt{m_0} \tag{1}$$

where m_0 is the area under the encountered wave height spectrum.

Considering the fact that the hull response is frequency dependent, a smoothed Power Spectrum Density (PSD) for the encountered wave height and motion are obtained by applying Fast Fourier Transform (FFT) with Welch's method (8000 samples Blackman-Harris 50% overlap windowing).

The heave RAO and angular RAOs, i.e., pitch and roll RAO, are defined as equations (2) and (3) respectively.

$$\text{Heave } RAO = \sqrt{\frac{\text{Encountered heave PSD}}{\text{Encountered wave height PSD}}} \tag{2}$$

$$\text{Angular } RAO = \sqrt{\frac{\text{Encountered angular motion PSD}}{\text{Encountered wave slope PSD}}} \tag{3}$$

The encountered wave slope PSD of the n^{th} sine wave FFT component in irregular waves is calculated as $\alpha_n = k_n \varsigma_n$, where α_n is the n^{th} wave slope, k_n is the n^{th} wave number, and ς_n is the n^{th} wave amplitude. In the region of sea trials, the minimum water depth was about 130 m [51], which means it could be considered deep water for the waves shorter than 260 m [52]. Thus, the sea trials were completed in deep water, and hence $k_n = \omega_n^2/g$, where ω_n is the n^{th} wave component frequency and g is gravitational acceleration. Also consider that $k_n = 2\pi/\lambda_n$, where λ_n is the n^{th} wave length. Therefore, the wave slope PSD can be estimated by equation (4), which is valid for all the waves frequencies higher than 0.5 rad/s during the trials.

$$\text{Encountered wave slope PSD} = \frac{\omega_n^4}{g^2}\text{Encountered Wave height PSD} \tag{4}$$

The dimensionless wave encounter frequency ϖ_e^* is $\varpi_e^* = 2\pi f_e\sqrt{L_{WL}/g}$, where the encounter frequency f_e is in Hz and L_{WL} is the length of vessel water-line.

According to ISO-2631-1 [46], MSI can be estimated by $MSI = K_m a_w \sqrt{T_e}$, where K_m is the constant 1/3, suggested by the ISO for a mixed population of unadapted males and females; a_w is the root mean square of frequency-weighted vertical acceleration, $a_w = [\sum_i (W_i a_i)^2]^{0.5}$; T_e is the exposure time in seconds; W_i is the frequency dependent weighting factor defined in the ISO standard; and a_i is the root mean square acceleration for the i^{th} one-third octave.

The spatial shift method suggested by Lau, Ali-Lavroff [38] for the time-domain vertical accelerations is also used in the present study to estimate the MSI distribution in the passenger cabin. It is based on the instantaneous accelerations recorded at LCG and bridge, the difference of their longitudinal locations, and the measured roll angle.

3 Results and discussion

3.1 Time records of sea trials data

The typical time traces of HSV-2 Swift sea trials data are shown in the Figure 4, which consists of two run conditions of deployed and retracted T-foil. Both datasets were recorded at a 2.1 m significant wave height in bow quartering seas (heading 135 and 225 degrees) at 35 knots or Froude Number (Fr) = 0.6. The plot consists of ship motion and ride control activity including instantaneous wave elevation at bow, heave displacement, angular displacements, and their rates at the LCG, and the activity of the ride control actuators. The parameters are divided by their own extreme magnitudes in order to be normalised and presented in the range of -1 to 1, and time is normalised by the factor $\sqrt{L_{WL}/g}$. These records contain crucial information on the external excitation, ride control activities and how the vessel responds. A zero-phase noise filter (4th order Butterworth with cut off at 0.5 Hz) is applied to all datasets in the plot.

The left-hand side shows the activity of the T-foil and stern tabs when the T-foil was deployed, whereas the right-hand side demonstrates the case of T-foil retracted out of the water. It should be noted that the stern tabs were still programmed to actively counter pitch and roll vessel motion when the T-foil was retracted.

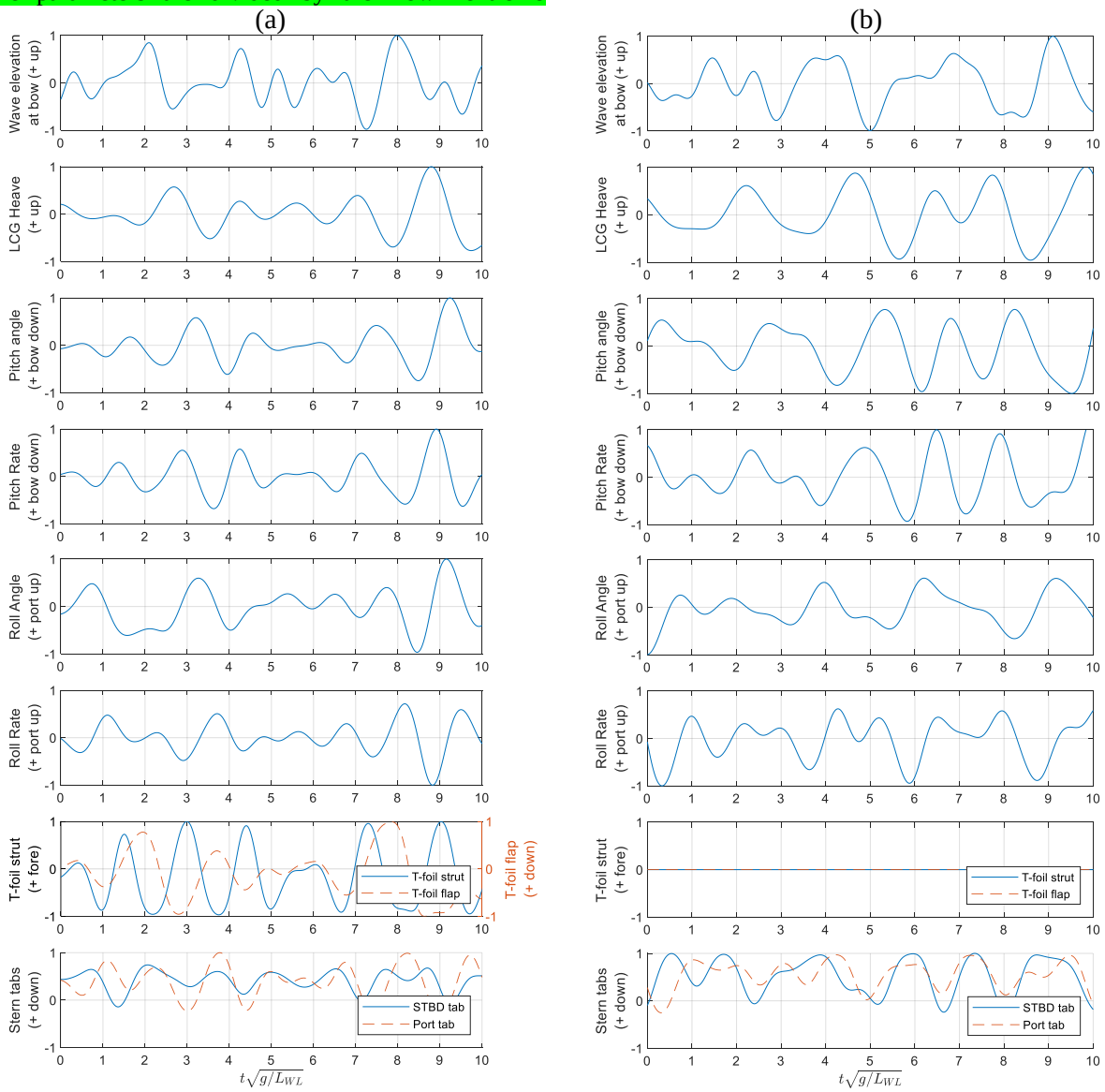

Figure 4: Normalised ship motion and ride-control activity recorded during sea trials of HSV-2 98m Incat Wave Piercing Catamaran in bow quartering seas (heading 135 and 225 degrees) with a 2.1 m significant wave height at a speed of 35 knots (Fr=0.6) (a) T-foil deployed with stern tabs (b) Stern tabs only.

3.2 Influence of T-foil deployment on vessel motions at various speeds

According to ISO standard 2631-1 [46], MSI highly depends on the environmental vertical accelerations, which means the heave and pitch motion on an advancing vessel are the key factors for passenger comfort. Therefore, heave and pitch RAOs are analysed in this section. Moreover, since rolling response is significant in oblique seas headings, the roll RAO affects vertical motions and is considered for locations off the centreline. All three RAOs are based on the data records, i.e. vertical acceleration (by double integral) and angular orientations, measured at the LCG.

To visualise the method of RAO evaluation in the present study for those measurements recorded in the irregular seas, sample plots of the unsmoothed and smoothed signals are presented in Figure 5. The smoothed ship motions PSD, i.e. heave, pitch, and roll are plotted with solid lines, using the smoothing method that has been described in section 2.3. Superimposed on that, the unsmoothed motions PSD are bar-plotted in black. Since the number of data points (bins) depends on the record data number, there are more than 60000 data points across the spectrum for our shortest records (20 minute record sampled at 100 Hz). There are more than 300 points within the range of frequencies of interest, i.e. $2 \leq \omega_e^* \leq 6.5$. These ship response PSDs are plotted along with the smoothed PSD of the environmental excitements, i.e. encountered wave height and slope. As described in section 2.3, the RAOs of heave, pitch, and roll are calculated based on the smoothed PSD of the ship motions as well as environmental inputs.

Figure 6 shows the trend of RAO reduction due to T-foil deployment in bow quartering seas, by comparing the cases of T-foil with stern tabs and the cases of stern tabs only. At high speed and low frequencies, i.e. $\omega_e^* < 4$, a general reduction can be observed in both heave and pitch RAOs. On the other hand, at high frequencies, i.e. $\omega_e^* \geq 4$, there is less difference in both heave and pitch RAO, regardless of the advancing speed.

It is worth mentioning that the pitch RAO in oblique seas is lower than that in head seas at low frequencies. In head seas at the higher speed case, the pitch RAO at low wave encounter frequencies is about 0.9 to 1.1 [38], while in oblique seas it is only around 0.6 to 0.9. This observation is easy to understand as a significant portion of encountered wave energy in oblique headings excites roll motion, instead of only pitch in head seas.

Finally, it should be noted that the relative wave heading is only judged by visual observation at the beginning of each trial, while in the actual world, the direction of waves, winds and swells in the sea trial region are unlikely to be purely unidirectional, or to remain constant throughout the recording duration. The influence of environmental factors should particularly be kept in mind when reading the angular RAOs, which were strongly dependent to the actual encountered heading angle in particular the roll RAO.

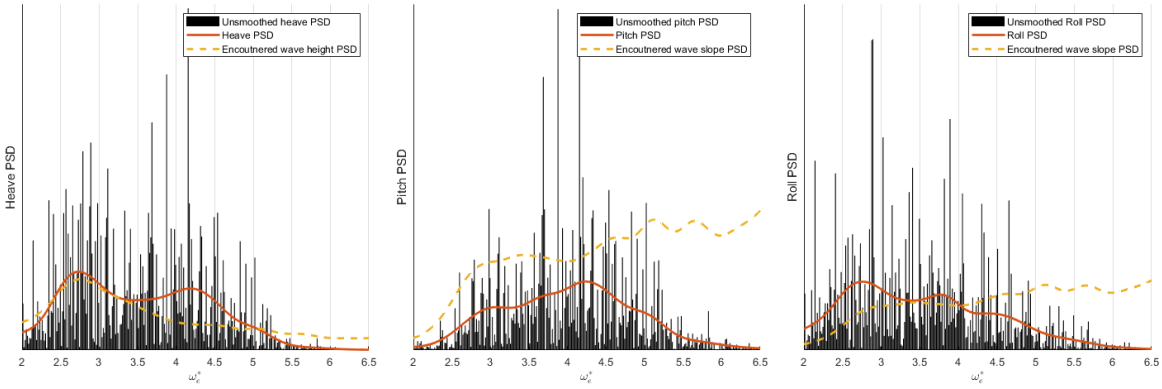

Figure 5: Sample of ship motion and environmental power spectrum density of HSV-2 Swift in bow quartering seas at 30 knots

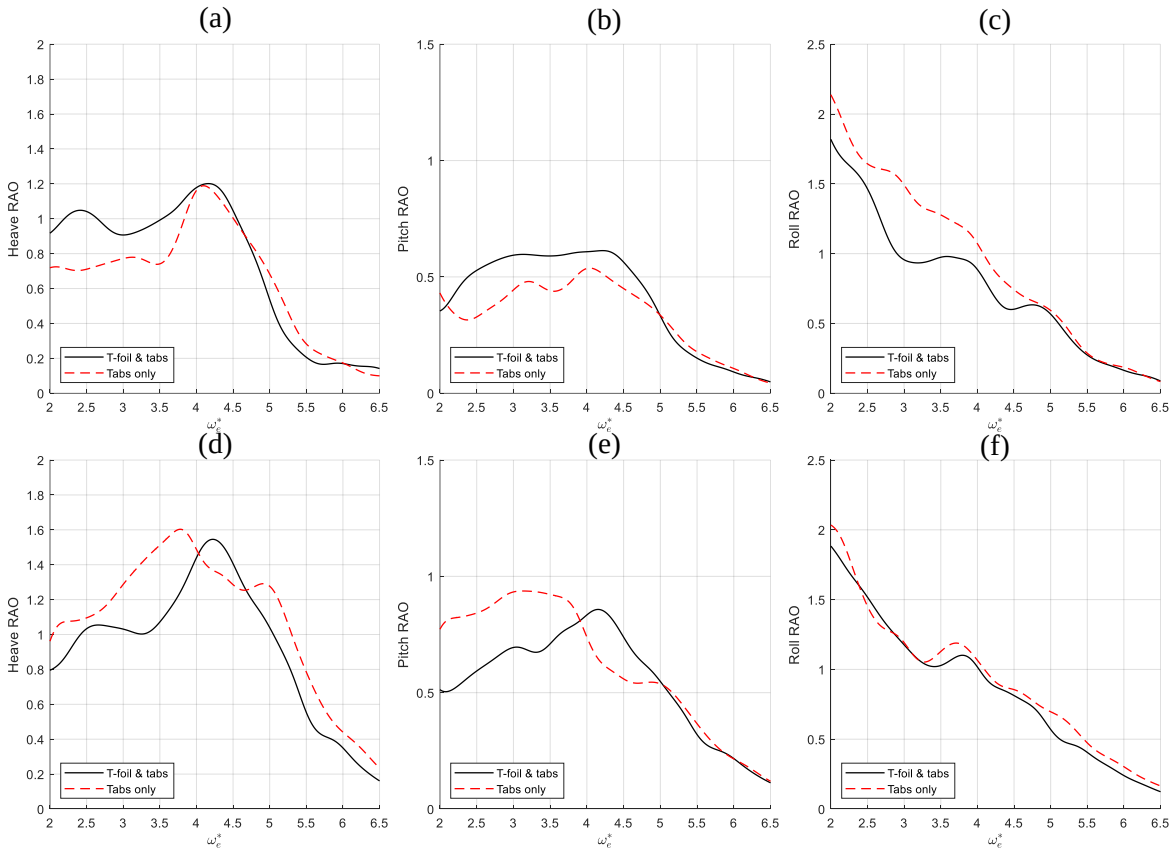

Figure 6: Response amplitude operators with T-foil and without T-foil of HSV-2 Swift in bow quartering seas at various speeds. (a) Heave RAO at 20-knots; (b) Pitch RAO at 20-knots; (c) Roll RAO at 20-knots; (d) Heave RAO at 30-knots; (e) Pitch RAO at 30-knots; (f) Roll RAO at 30-knots.

3.3 Motion sickness incidence at different headings

The influence of headings on Motion Sickness Incidence (MSI) is shown in Figure 7. As discussed in Section 2.3, MSI here is based on the method described in ISO-2631-1 [46], The MSIs shown in Fig.7 are normalised values for better illustration, i.e. the MSI values are divided by the maximum MSI value at high speed.

From both plots, a similar range of MSI values can be observed in head seas and oblique seas. A normalised MSI of about 0.5 is found in both headings at low speed (15-20 knots, Fr≈0.3) (Figure 7 (a)), while it is around 0.9 at high speed (30-35 knots, Fr≈0.6) (Figure 7 (b). This agrees with the prediction of Fang and Chan [16] that the WPC heave response was consistent in the range of headings $180° \pm 45°$ at the same forward velocity.

In a previous study by the authors using the same sea trials data [38], which analysed the single speed of 35 knots, the MSI in bow-quartering seas was found to be generally only half of that in head seas. However, there were limited runs at this specific speed, and this was not found to be the case if more runs were considered by broadening the selection to speeds in the range 30-35 knots. Since the sea trials were performed in the real world, there were many factors that could affect MSI estimation, for example, the existence of secondary waves and varying vessel displacement. By including additional cases with similar speeds in the present study, this could reduce the influence of a single case that may mislead the conclusions.

In Figure 7 (a), a minor reduction in the normalised MSI caused by deployment of the T-foil is found regardless of the headings. By comparing the cases with *Hs* in the range of 1.75 to 2 m, percentage reductions of 8% and 7% are observed in head and oblique seas respectively.

Furthermore, a MSI reduction due to T-foil deployment is observed in Figure 7 (b). In head seas, MSI is reduced by 22% in the group of *Hs* from 2.25 to 2.55 m. Similarly, there was about 13% reduction in bow quartering seas at high speed (30-35 knots, Fr≈0.6). As expected, the RCS effectiveness in reducing MSI at high speed is very notable compared with the case at low speed. This can easily be explained by the larger lift force that can be generated by the T-foil at higher speed. The percentage reduction for two headings and speeds have been summarised in Table 2, which shows that the capability of RCS at 30-35 knots is doubled or even more, in both head sea and oblique sea headings, relative to the lower speed (15-20 knots, Fr≈0.3).

The reductions in both headings are given in the table, showing that the reductions in head seas exceeded that in oblique seas, regardless of the speed. This is most likely because the T-foil was fitted on the centre line of the vessel, which meant it can be effective in controlling heave and pitch motions, but not rolling. Considering that roll motion is the dominant response when the vessel encounters waves from the bow quarter, it is not unexpected to find the effectiveness of the T-foil in oblique seas is not as significant as in head-seas.

The trend in the heave motion reduction due to T-foil and speed align with previous studies [9, 53], but the present study is the first to quantify the RCS effectiveness, and the influences of the heading and speed on MSI based on full-scale sea trials investigation. These values provide a sound reference for comparison in future studies of the RCS effectiveness on WPCs.

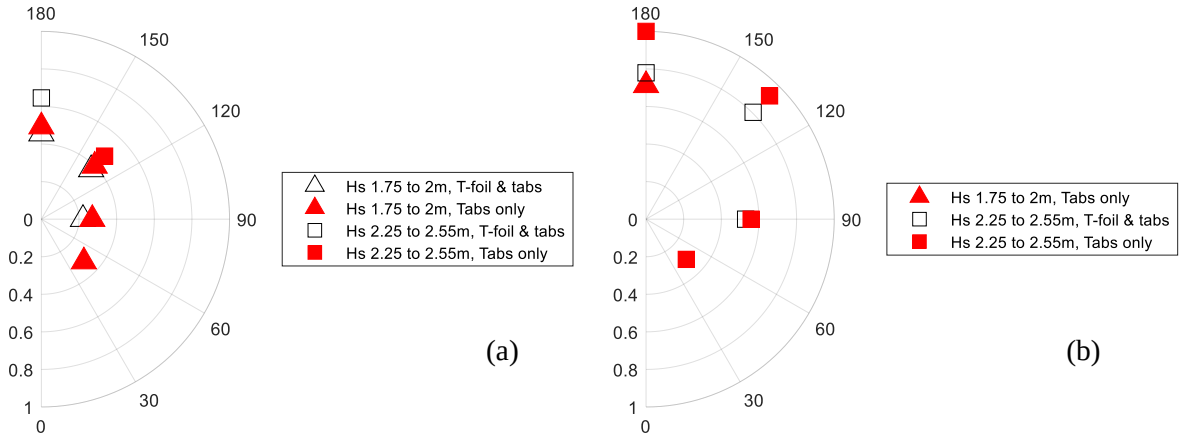

Figure 7: Normalised MSI in different headings in sea trials at (a) 15-20 knots (Fr≈0.3) (b) 30-35 knots (Fr≈0.6), grouped by significant wave height and Ride Control System (RCS) activation (Port mirrored to starboard)

Table 2: Percentage reduction of MSI by T-foil deployment (with stern tabs remaining active) at various headings and vessel speeds, and the ratio of the reduction in MSI caused by vessel speed

	Head sea	Bow quartering sea
Low speed (Fr ≈ 0.3)	8%	7%
High speed (Fr ≈ 0.6)	22%	13%
High speed/low speed (Ratio)	2.8	1.9

3.4 Regression model fitting MSI in oblique seas

In Section 3.3, by comparing eight different cases, the ratio of the MSI reduction caused by T-foil deployment, headings, and speeds are quantified. Although the estimated reductions agree well with expectation, considering that there were many random factors potentially affecting the vessel motion during the sea trials, the foundation of the RCS effectiveness estimation need to be widened before reaching a conclusion. Therefore, in this section, more sea trial records were considered and fitted into regression models for a better analysis.

To further reduce the influence of random error in each sea trial run, the sea trials data were segmented into 10-minute windows, with 50% overlap. For each segment of the record, the MSI was assessed individually from the acceleration measured at the LCG by the method in ISO-2631-1 [46]. By grouping the sea trial records into high speed, i.e. 30-35 knots (Fr≈0.6), and low speed, i.e. 15-20 knots (Fr ≈ 0.3), two regression models were fitted for MSI as the dependent variable as a function of significant wave height (*Hs*), encountered peak wave frequency (*Fp*), and T-foil deployment.

Based on 36 observations in oblique seas at the speed of 30 to 35 knots, the regression model was fitted with coefficient of determination (R^2) = 0.790, adjusted R^2 = 0.763. In Figure 8 (a), the cases of T-foil with stern tabs are plotted as small black markers, and the MSI values of stern tabs only cases are shown in large red markers. The fitted model is visualised as two surfaces, T-foil retracted (upper surface) and deployed (lower surface) separately.

According to the mathematical model, the MSI value most strongly depends on *Hs* (p=6.2×10^{-8}), *Fp* (p=0.0002), and F_p^2 (p=0.0005). The effect of T-foil deployment (p=0.001) is also identified in the model.

The MSI percentage reduction due to T-foil deployment varies from about 15% up to 50%, depending on the magnitude of the denominator, as shown in Figure 8 (b). On average, a 21% MSI reduction by deployment of an active T-foil at high speed is found. Overall, in terms of estimated MSI reduction, the ability of the T-foil remains essentially unchanged with varying *Hs* and *Fp*, while the MSI percentage reduction becomes significant (up to 50%) with low MSI value.

Next, the low-speed oblique sea model was built based on 15 observations, and the regression model (Figure 9 (a)) was fitted with coefficient of determination (R^2) = 0.981, adjusted R^2 = 0.974.

In the model for the speed range of 15 to 20 knots, the MSI was also dependent on *Hs* (p=2.5×10^{-7}), *Fp* (p=0.0003), F_p^2 (p=0.0009), and T-foil deployment (p=1.1×10^{-7}). Like the high-speed model, the ability of RCS is found to be independent to the encountered wave height and spectrum at low velocity. Moreover, the MSI percentage reduction remains relatively constant at the mean value of about 11% for the lower speed case.

By comparing the estimated MSI reduction in section 3.3 and 3.4, there are both common and disparate features between the predictions.

First, the reduction due to an active T-foil at high speed (Fr≈0.6) in oblique sea is about double the amount of low speed (Fr≈0.3). This observation is valid in both the normalised MSI plots and regression models. From the normalised polar plot, the MSI percentage reduction is 13% at high speed, while the reduction is limited to 7% at low speed. Similarly, the predicted average reductions are 21% and 11% in the regression models at high and low speed respectively.

Nevertheless, there is a difference between the average percentage reduction estimated by the models and normalised MSI plots, e.g. 21% compared to 13% at high speed. Considering the sea trials were performed in an open environment, there were again many uncontrollable elements that could affect the measured data, so the ability to draw precise quantitative conclusions from a very limited number of observations of course will contain a limited amount of uncertainty. Also, since the mathematical models are only derived over the range of conditions, e.g., speed, significant wave height, and encountered peak wave frequency, that are presented in the plots, this limitation should be kept in mind. Further research is required before extrapolating outside the specific range.

However, since full scale sea trials records are very valuable for analysing the seakeeping performance, and also the deviated models demonstrate interesting features regarding the effectiveness of the RCS as a

function of speed along with encountering waves, these reveals could benefit from the development of RCS to further increase WPC passenger comfort.

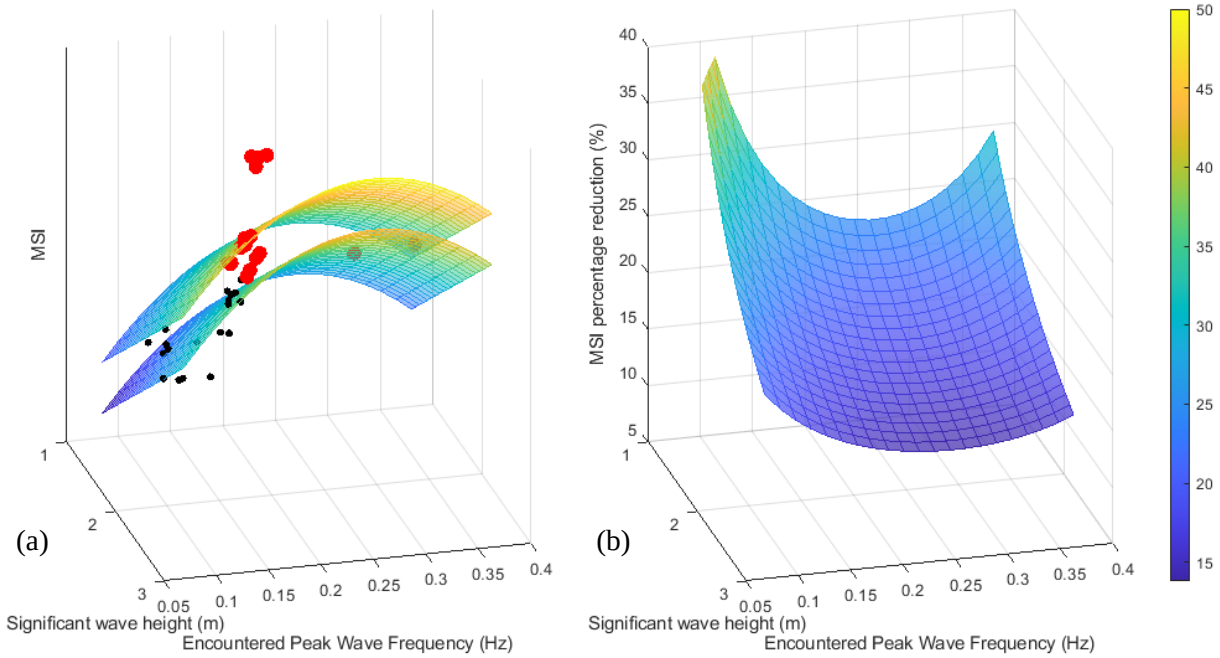

Figure 8: 3-D plot of MSI with T-foil and tabs deployed (small, black markers: regression model lower surface), and with stern tabs only (large, red markers: regression model upper surface) (b) 3-D plot of MSI percentage reduction due to T-foil deployment in oblique seas at 30-35 knots (Fr≈0.6)

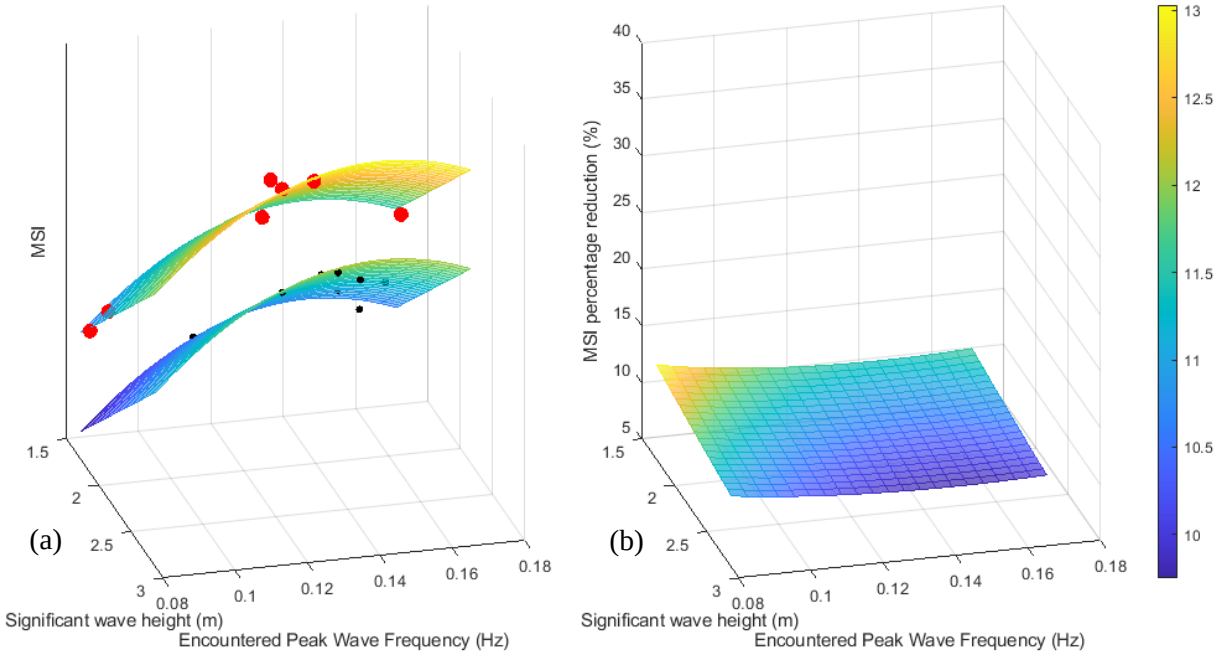

Figure 9: 3-D plot of MSI with T-foil and tabs deployed (small, black markers: regression model lower surface), and with stern tabs only (large, red markers: regression model upper surface) (b) 3-D plot of MSI percentage reduction due to T-foil deployment in oblique seas at 15-20 knots (Fr≈0.6)

3.5 MSI throughout the passenger cabin

Since the purpose of MSI assessment is to obtain insight into the reaction of ordinary population to vessel motion [46], it is most meaningful to estimate the MSI inside the passenger cabin, rather that at the extremities of the vessel. During the sea trials, although there were four accelerometers installed on the catamaran, none of them was on the passenger deck. Therefore, in the present study the accelerations were extrapolated to different locations in the cabin by the time-domain spatial shift method [38], and by this method, the distribution of MSI in the passenger cabin was evaluated. The X (longitudinal) and Y (transverse) coordinates were based on the general arrangement of the HSV-2 Swift vessel. X = 0 m is set at the transom, and Y = 0 m represents the centreline of the ship.

The MSI distribution of the case of stern tabs only in 2.7 m bow-port sea at 35 knots (Fr=0.6) is plotted in Figure 10 (a). As would be expected, the highest MSI can be found at the corner of the cabin encountering waves, i.e. port fore. The normalised MSI drops to about 0.8 at the starboard fore corner, and about only half of the highest MSI at the aft region. Both of these observations are reasonable and agree with the findings at a speed of 30 knots [38].

Figure 10 (b) illustrates the percentage reduction of MSI on the deployment of the active T-foil. The reduction is calculated by comparing the case shows in Figure 10 (a) along with a T-foil deployed with stern tabs case (35 knots; bow quartering; *Hs* = 2.4 m). It is easily seen that the X location dominates the effectiveness of RCS, for instance, the highest reductions are 23% aft of the cabin, and about 22% at the LCG (X ~ 40 m). This agrees with the previous analysis for the reduction (21%) at the location of LCG in section 3.4. The influence of the T-foil deployment declines with the increasing longitudinal coordinate, such that at the fore of the cabin, there is no significant reduction in MSI. This could be explained by the larger denominator, i.e. higher MSI magnitude, at the fore of the cabin. Overall, there was a 10% reduction on average throughout the entire passenger cabin, by comparing the cases of active T-foil with stern tabs and the cases of stern tabs only.

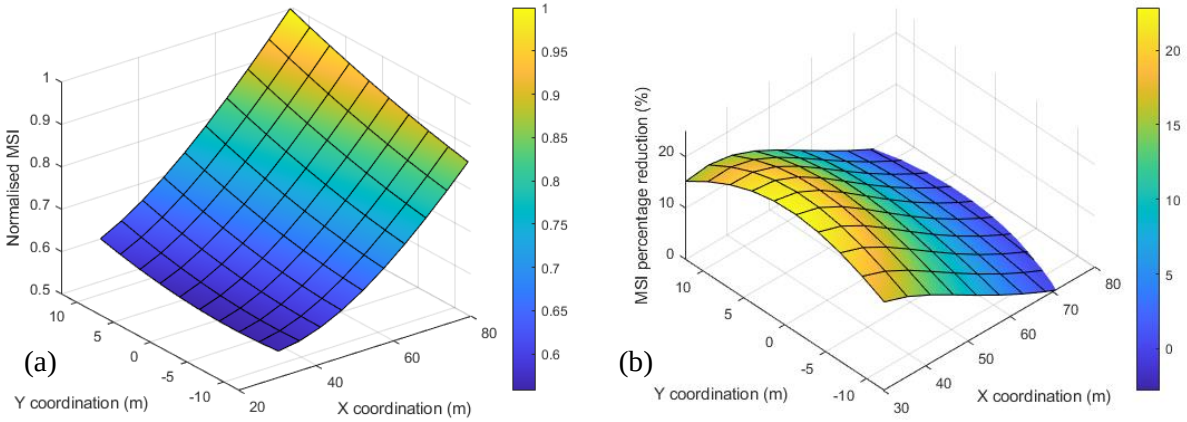

Figure 10: 98m WPC passenger cabin: (a) MSI distribution (stern tabs only with T-foil retracted) (b) MSI percentage reduction with deployment of the active T-foil (in addition to stern tabs) at 35 knots (Fr=0.6) with significant wave height of 2.4 and 2.7 m in bow quartering seas (Starboard mirrored to port for valid comparison)

4 Conclusions

Sea trial records for a 98 m Wave-Piercing Catamaran (WPC), HSV-2 Swift, were analysed to investigate the influence of deploying an active T-foil on vessel motion response and the effects on passenger comfort. This Incat Tasmania catamaran was fitted with a retractable T-foil located aft of the centre bow, and two trim tabs at the stern of the demi-hulls. The stern tabs were always programmed to actively counterbalance the pitch and roll motion in damping control throughout the sea trials, while the T-foil could be actively deployed or retracted. Thus, the effect on vessel motion of the T-foil deployment with stern tabs was assessed in this study, based on full-scale WPC in oblique seas with random waves.

Heave, pitch and roll motion Response Amplitude Operators (RAO) were analysed and compared with previous sea trial studies. A comparison of the cases of stern tabs only and T-foil with tabs active showed that both the heave and pitch RAOs were reduced at low frequencies (ω_e^*<4, 0.2 Hz). The reductions improved with greater forward speed. However, the pitch RAOs in oblique seas were lower than in head seas at low frequencies regardless of the velocity.

Motion Sickness Incidence (MSI) in different headings were studied at high speed (30-35 knots, Fr≈0.6) and low speed (15-20 knots, Fr ≈ 0.3). As expected, the effect of T-foil deployment in bow-quartering seas was limited compared to the cases in head seas. In terms of MSI percentage reduction, the T-foil was found to be twice as effective on reducing MSI at high speed (13%) than at low speed (7%).

To generalise the impact of random factors in the sea trials, regression models were fitted to the oblique seas MSI as a function of significant wave height (*Hs*) and encountered peak wave frequency (*Fp*). The model showed the RCS effectiveness to be largely independent of the encountered wave height and frequency, but highly dependent on the speed. Consistent with previous observation, the effectiveness of T-foil in reducing MSI increased with speed in oblique seas, where the average reduction at high speed is about twice that at low speed (21% vs. 11%).

Finally, the MSI in the passenger cabin was investigated in oblique seas by a time-domain spatial shift method. Unsurprisingly, the highest normalised MSI was found at the cabin corner facing the encountered waves. The MSI declined along the vessel, down to about only half of the MSI at aft region at the foremost edge opposite to the encountered wave direction.

Overall, the conclusions from the sea trial records in oblique seas show good alignment with those in a related previous sea trials study [38], towing tank work [26] and numerical analyses [5, 15]. The present study also quantified the effectiveness of the active T-foil deployment in various conditions, more specifically, the MSI percentage reduction at high-speed was double that at low speed, and motions reduced by the T-foil are much more significant in head seas than in oblique seas.

Acknowledgements

The authors wish to thank Incat Tasmania Pty Ltd and Revolution Design Pty Ltd, especially Dr Jason McVicar, for direct input towards this research. Naval Surface Warfare Center, Carderock Division (NSWCCD) is also acknowledged for providing access to data collected from HSV-2 Swift sea trials. The Australian Research Council (ARC) is also gratefully acknowledged in supporting this work thru Linkage grant LP 1701000555.

References

1. Yun L and Bliault A. Features of High Speed Catamarans; Wave Piercing Catamarans; Trimarans. *High Performance Marine Vessels*. 2012, pp.209-240.
2. Veer APvt. *Behaviour of catamarans in waves*. Delft University of Technology, Netherlands, 1998.
3. AlaviMehr J, Lavroff J, Davis MR, et al. An experimental investigation of ride control algorithms for high-speed catamarans Part 2: Mitigation of wave impact loads. *Journal of Ship Research* 2017; 61: 1-13. Refereed Article. DOI: 10.5957/JOSR.61.2.160046.
4. Tezdogan T, Incecik A and Turan O. Operability assessment of high speed passenger ships based on human comfort criteria. *Ocean Engineering* 2014; 89: 32-52.
5. Davis MR. Operation of T-Foils and Stern Tabs to Improve Passenger Comfort on High-Speed Ferries. *Journal of Ship Research* 2021; 1.
6. Hu K, Ding Y and Wang H. High-Speed Catamaran's Longitudinal Motion Attenuation with Active Hydrofoils. *Polish Maritime Research* 2018; 25: 56-61.
7. He W, Yang S, Xie W, et al. Research on Motion Reduction of a T-Foil on the Wave Piercing Catamaran. *2nd International Conference on Frontiers of Materials Synthesis and Processing*. IOP Publishing, 2019.
8. Holloway DS and Davis MR. Ship motion using a high Froude number time domain strip

theory. *Journal of Ship Research* 2006; 50: 15-30. Refereed Article.
9. Jiang Y, Bai J, Sun Y, et al. Numerical investigation of T-Foil hybrid control strategy for ship motion reduction in head seas. *Ocean Engineering* 2020; 217.
10. Zhang B and Ma S. Research on Motion Response and Sickness Incidence of the Fishing Boat in Heading and Quartering Seas. *Journal of FisheriesSciencescom* 2019; 13: 26-33.
11. Shabani B, Lavroff J, Holloway DS, et al. The influence of the centre bow and wet-deck geometry on motions of wave-piercing catamarans. *Journal of Engineering for the Maritime Environment* 2019; 232: 474-487. Refereed Article. DOI: 10.1177/1475090217753761.
12. AlaviMehr J, Davis MR, Holloway DS, et al. Optimisation of ride control operation to reduce motions and loads of high-speed catamarans. *14th International Conference on Fast Sea Transportation*. Nantes, France2017, p. 215-222.
13. Fang CC, Chan HS and Incecik A. Investigation of motions of catamarans in regular waves-I. *Ocean Engineering* 1996; 23: 89-105.
14. Fang CC, Chan HS and Incecik A. Investigation of motions of catamarans in regular waves—II. *Ocean Engineering* 1997; 24: 949-966. DOI: https://www.sciencedirect.com/science/article/pii/S0029801897000565?via%3Dihub.
15. Fang C-C and Chan H-S. An investigation on the vertical motion sickness characteristics of a high-speed catamaran ferry. *Ocean Engineering* 2007; 34: 1909–1917.
16. Fang C-C and Chan H-S. Investigation of seakeeping characteristics of high-speed catamarans in waves. *Journal of Marine Science and Technology* 2004; 12: 7-15.
17. ShipTechnology. Francisco High-Speed Ferry, https://www.ship-technology.com/projects/francisco-high-speed-ferry/ (2012, accessed 3 2020).
18. O'Hanlon JF and McCauley ME. Motion Sickness Incidence as a Function of the Frequency and Acceleration of Vertical Sinusodal Motion. *Aerospace Medicine* 1974; 45: 366-369.
19. McCauley ME, Royal JW, Wylie CD, et al. *Motion sickness incidence exploratory studies of habituation, pitch and roll, and the refinement of a mathematical model*. 1976. California: Office of naval research department of the navy.
20. Cruz JMDl, Aranda J, Giron-Sierra JM, et al. Improving the comfort of a fast ferry. *IEEE Control Systems Magazine* 2004.
21. Stevens SC and Parsons MG. Effects of Motion at Sea on Crew Performance: A Survey. *Marine Technology* 2002; 39: 29-47.
22. Giron-Sierra JM, Esteban S, De Andres B, et al. Experimental study of controlled flaps and T-foil for comfort improvement of a fast ferry. 2000.
23. Riola JM, Esteban S, Giron-Sierra JM, et al. Motion and Seasickness of Fast Warships. *RTO AVT Symposium*. Prague, Czech Republic2004.
24. Davis MR and Holloway DS. Effect Of Sea, Ride Controls, Hull Form And Spacing On Motion And Sickness Incidence For High Speed Catamarans. In: Pasquale C, (ed.). *The 7th International Conference on Fast Sea Transportation*. Ischia (Italy): Arti GrafficheZaccaria SRL, 2003, p. E1-E10.
25. He W, Castiglione T, Kandasamy M, et al. Numerical analysis of the interference effects on resistance, sinkage and trim of a fast catamaran. *Journal of Maritime Science Technology* 2015; 20: 292-308.
26. AlaviMehr J, Lavroff J, Davis MR, et al. An experimental investigation of ride control algorithms for high-speed catamarans Part 1: Reduction of ship motions. *Journal of Ship Research* 2017; 61: 35-49. Refereed Article. DOI: 10.5957/JOSR.61.1.160041.
27. Gahlinger PM. Cabin location and the likelihood of motion sickness in cruise ship passengers. *Journal of Travel Medicine* 2000; 7: 120-124.
28. Almallah I, Lavroff J, Holloway DS, et al. Global load determination of high-speed wave-piercing catamarans using finite element method and linear least squares applied to sea trial strain measurements. *Journal of Marine Science and Technology* 2019: 1-13. Refereed Article. DOI: 10.1007/s00773-019-00688-3.
29. Thomas G, Winkler S, Davis M, et al. Slam events of high-speed catamarans in irregular waves. *Journal of Marine Science and Technology* 2011; 16: 8-21. Refereed Article. DOI: 10.1007/s00773-010-0105-y.
30. Davis MR, Thomas GA, Holloway DS, et al. Slamming and Whipping of Wave-Piercing Catamarans. In: Professor PT and Dr SEH, (eds.). *Hydroelasticity in Marine Technology*

International Conference. Southampton, UK: University of Southampton, 2009, p. on CD.
31. Shabani B, Lavroff J, Holloway DS, et al. The effect of centre bow and wet-deck geometry on wet-deck slamming loads and vertical bending moments of wave-piercing catamarans. *Ocean Engineering* 2018; 169: 401-417. Refereed Article. DOI: 10.1016/j.oceaneng.2018.09.028.
32. Shabani B, Holloway DS, Lavroff J, et al. Systematic model tests on centre bow design for motion and slamming load alleviation in high speed catamarans. *14th International Conference on Fast Sea Transportation*. Nantes, France2017, p. 136-143.
33. Shabani B, Lavroff J, Holloway DS, et al. Wet-deck slamming loads and pressures acting on wave piercing catamarans. *International Shipbuilding Progress* 2019; 66: 201-231. Refereed Article. DOI: 10.3233/ISP-180247.
34. Shabani B, Lavroff J, Holloway DS, et al. Centre bow and wet-deck design for motion and load reductions in wave piercing catamarans at medium speed. *Ships and Offshore Structures* 2019: 1-17. Refereed Article. DOI: 10.1080/17445302.2019.1708043.
35. AlaviMehr J, Davis MR, Lavroff J, et al. Response of a high-speed wave-piercing catamaran to an active ride control system. *Royal Institution of Naval Architects Transactions Part A International Journal of Maritime Engineering* 2016; 158: A325-A335. Refereed Article. DOI: 10.3940/rina.ijme.2016.a4.382.
36. Davis MR, Watson NL and Holloway DS. Measurement and prediction of wave loads on a high-speed catamaran fitted with active stern tabs. *Marine Structures* 2004; 17: 503-535. Refereed Article. DOI: 10.1016/j.marstruc.2005.01.003.
37. Matsubara S, Thomas G, Davis MR, et al. Influence of centrebow on motions and loads of high-speed catamarans. In: Peltzer TJ, (ed.). *11th International Conference on Fast Sea Transportation (FAST 2011)*. Honolulu, Hawaii: American Society of Naval Engineers, 2011, p. 661-668.
38. Lau C-Y, Ali-Lavroff J, Holloway DS, et al. Influence of active T-foil on motion response and passenger comfort of high-speed large wave-piercing catamaran by sea trials. *Journal of Marine Science and Technology* 2022. DOI: https://doi.org/10.1007/s00773-022-00876-8.
39. Shabani B, Lavroff J, Davis MR, et al. Slam loads and kinematics of wave-piercing catamarans during bow entry events in head seas. *Journal of Ship Research* 2018; 62: 134-155. Refereed Article. DOI: 10.5957/JOSR.180001.
40. Incat. HSV-2 Swift (Hull 61) specification, https://www.incat.com.au/vessel-progress/current-fleet/ (2003, 2021).
41. AlaviMehr J, Lavroff J, Davis MR, et al. An experimental investigation on slamming kinematics, impulse and energy transfer for high-speed catamarans equipped with Ride Control Systems. *Ocean Engineering* 2019; 178: 410-422. Refereed Article. DOI: 10.1016/j.oceaneng.2019.02.004.
42. Naiad. Active T-foils. Naiad Dynamics, 2020.
43. Smith N. *Identification of Ride Control System Parameters for a 98 Metre High Speed Catamaran*. University of Tasmania, Hobart, 2013.
44. Davis MR and Holloway DS. Motion and Passenger Discomfort on High Speed Catamarans in Oblique Seas. *International Shipbuilding Progress* 2003; 50: 333-370. Refereed Article.
45. Zhang S, Li S, Liang L, et al. Ride control method of Wave-piercing catamaran with T-foil and flaps. In: *International Conference on Mechatronics and Automation* Tianjin, China, 2014, IEEE.
46. ISO 2631-1:1997(E) Mechanical Vibration and Shock - Evaluation of Human Exposure to Whole-Body Vibration - Part 1 General Requirements.
47. Incat. Incat offical website, https://www.incat.com.au (2021, accessed 3 2021).
48. Bachman RJW, Dennis A. ; Powell, Mathew D. . HSV-2 Swift Seakeeping Trials. 2004.
49. Brady TF, Bachman RJ, Donnelly MJ, et al. *HSV-2 Swift Instrumentation and Technical Trials Plan*. 2004. Naval Surface Warfare Center.
50. TSK. Wave Height Meter. In: Co. T-S, (ed.). Kanagawa: Tsurumi-Seiki Co.
51. EMODnet. Bathymetry, https://portal.emodnet-bathymetry.eu/ (2021, accessed Apr 2021).
52. MIT. Water Waves. *Marine Hydrodynamics*. Massachusetts Institute of Technology - Department of Ocean Engineering, 2004.
53. Jacobi G, Thomas G, Davis MR, et al. Full-scale motions of a large high-speed catamaran:

the influence of wave environment, speed and ride control system. *International Journal of Maritime Engineering* 2012; 154: A143-A155. Refereed Article. DOI: 10.3940/rina.ijme.2012.a3.238.